

## Electron Conduction through Surface States of the Si(111)-(7 × 7) Surface

Seiji Heike,<sup>1,2</sup> S. Watanabe,<sup>3</sup> Y. Wada,<sup>1,2</sup> and T. Hashizume<sup>1</sup>

<sup>1</sup>Advanced Research Laboratory, Hitachi, Ltd., 2520 Akanuma, Hatoyama, Saitama 350-0395, Japan

<sup>2</sup>CREST, Japan Science and Technology Corporation (JST), 2520 Akanuma, Hatoyama, Saitama 350-0395, Japan

<sup>3</sup>Department of Material Science, The University of Tokyo, Hongo, Bunkyo-ku, Tokyo 113-8656, Japan  
(Received 23 January 1998)

Electronic properties of the Si(111)-(7 × 7) surface are evaluated by scanning tunneling microscopy/spectroscopy (STM/STS) using artificially fabricated insulating trenches. When the surface is surrounded by a closed trench, the effect of the Schottky barrier naturally formed between the surface states and the bulk states is observed by STM. When a half-closed tape-shaped structure surrounded by the trench is fabricated, the current path is dominated by that through surface states. Its conductivity is estimated by measuring the voltage drop along the structure. [S0031-9007(98)06730-1]

PACS numbers: 73.20.At, 61.16.Ch, 73.25.+i, 73.30.+y

For the downscaling of electronic devices, investigating surface electronic properties is of great importance because the surface effects become larger as their scale becomes smaller. Electron transport through surface states has long been investigated [1]. The surface-state conductivity of a Si(111) cleaved surface was estimated first by Aspnes and Handler from measurement of the sample conductance, and the reported value was negligibly small [2]. Later, Persson deduced the surface resistivity of Si(111)-(7 × 7) using electron-energy-loss spectroscopy (EELS) data [3]. In the last ten years, the surface states of metals and semiconductors have been studied using scanning tunneling microscopy/spectroscopy (STM/STS) [4]. Hasegawa *et al.* reported the electron standing waves observed on the surface steps of Au(111) due to scattering of the surface-state electrons at the step edges [5]. Eigler *et al.* observed surface-state standing waves confined in an artificially fabricated quantum corral on a Cu(111) surface [6]. The conductance of a Si(111)-(7 × 7) surface was estimated from nanoscale point contact of the STM tip on the surface by Hasegawa *et al.* [7]. However, electron conduction through surface states has not yet been detected directly by experiment.

In this Letter, we used the surface modification technique [8] to fabricate trench patterns and investigated the electronic properties of the Si(111)-(7 × 7) surface using a current flowing between the STM tip and the surface. A semiconductive band gap was observed by STS in the trench region, which means that the current path through metallic surface states is cut by the trench. We found that the direct current path from the surface states to the bulk states was hindered at a positive sample bias. Thus we could control the current path of surface-state conduction by forming designed insulating trenches. We measured the voltage drop generated by the surface current along a tape structure and estimated the conductivity through the surface states of the Si(111)-(7 × 7) surface for the first time.

The STM used in this study is a homemade system in an ultra-high-vacuum (UHV) chamber with a base

pressure of  $7 \times 10^{-11}$  Torr. An *n*-type 0.005- $\Omega$  cm Si(111) sample was outgassed at 700 °C overnight and was annealed at 1250 °C for 5 s to obtain a Si(111)-(7 × 7) surface. All these procedures were performed in a sample preparation chamber with a pressure in the low  $10^{-10}$ -Torr range. Probe tips were prepared by electrochemical etching of tungsten wires and heating by electron bombardment in UHV. All the trench patterns were formed by moving the tip along the surface at a constant tunneling current of 100 to 300 nA and a sample bias of -3.0 V [8].

Figures 1(a) and 1(b) show STM images of a 100-nm-diam circular trench pattern observed at a current of 1.0 nA and at sample bias voltages of -2.0 and +2.0 V, respectively. The corresponding cross-sectional views along the dashed lines are also shown. For the closed trench pattern, the inside region was observed 0.02 nm lower than the outside region for negative bias and 0.08 nm lower for positive bias. The apparent height change is more remarkable at a positive voltage, for a lower sample bias, and for a larger tunneling current. This tendency indicates that the height changes are not attributed to a structural change. A similar effect has been observed inside an insulating DNA loop due to a lowering of conductance [9]. The present phenomenon can also be explained similarly, but a simple conductance drop due to the trench cannot explain the asymmetric behavior of the STM observation, as will be discussed later. The most plausible explanation is based on the Schottky barrier (SB) naturally formed between the surface states and the bulk, as shown in Fig. 1(c). The surface Fermi level is pinned by the dangling-bond states on the surface, and band bending at the subsurface region [10] results in SB formation.

The electronic structure of the trench itself was investigated by STS. A clear band gap of approximately 1.4 eV is observed for the trench region [Fig. 1(d)], which indicates that no surface state exists on the trench. The dangling bonds generated after removal of Si atoms [11] must be passivated by other atoms, e.g., oxygen, hydrogen, and others. At this stage, the surface modification mechanism

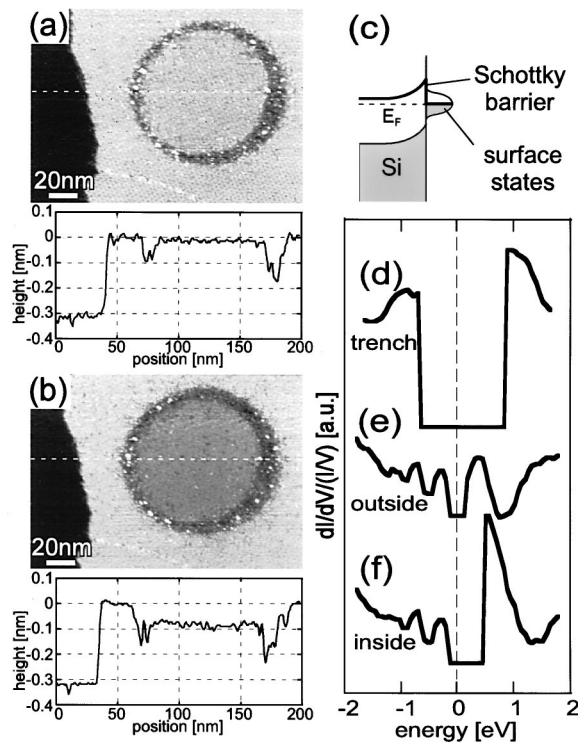


FIG. 1. STM images of a 100-nm-diam circle pattern observed at sample bias voltages of (a)  $-2.0$  V and (b)  $+2.0$  V and at a tunneling current of  $1$  nA, and the corresponding cross-sectional views. The surface inside the circle is observed  $0.02$  nm lower in (a) and  $0.08$  nm lower in (b) than the outside region. (c) A schematic energy band diagram of the natural Schottky barrier between the surface states and the bulk states. Tunneling spectra (d) on the trench, (e) outside the pattern, and (f) inside the pattern were measured. The tunneling gap was stabilized at  $-2.0$  V and  $1.0$  nA. No surface states exist on the trench region. The empty-state electronic structure is shifted towards higher energy inside the circle.

and the structure of the trench region are not clear and will be discussed elsewhere. The spectrum of the surface outside the circle [Fig. 1(e)] shows a typical electronic structure of a Si(111)-(7  $\times$  7) dimer-atom–stacking-fault (DAS) structure [12]. It shows three clear peaks corresponding to the occupied and unoccupied states of adatoms and the occupied state of rest atoms [13]. The electronic structure inside the circle above Fermi energy ( $E_F$ ) appears to be shifted towards higher energy, while the spectrum below  $E_F$  is almost the same as that of the outside region [Fig. 1(f)]. A gaplike structure also appears from  $E_F$  to  $0.5$  eV. This tunneling spectra showing rectifying characteristics can be understood by the SB formation between the surface states and the bulk.

When the SB is reverse biased at a positive voltage, the thermionic current [14] through the SB is negligibly small. At a negative sample bias, the resistance across the surface-bulk interface is relatively small because the SB is forward biased. In addition to the thermionic current, there are two current leakage paths from the surface states to the bulk (the corresponding resistance is defined

here as a leakage resistance  $R_{\text{leak}}$ ). One is the current through the trench due to the finite resistance of the trench region. The other is the current through the surface-bulk interface including a tunneling current through the SB and a ballistic current originating from electrons injected by the tip [15]. Consequently, the current through these leakage paths generates a voltage between the surface inside the circle and the bulk, which lowers the effective sample bias inside the circle. As a result, the tip-surface distance becomes smaller to keep the current constant, and the apparent height inside the circle is reduced in the STM images.

When the tip is outside the trench at a positive bias voltage, the tunneling electrons scattered at the surface-bulk interface [16] can travel along the surface-state layer which spreads infinitely along the surface outside the trench. The electrons eventually leak into the bulk by the leakage path through the surface-bulk interface. So the total resistance for the electrons before reaching the bulk is low and the voltage drop is negligible. The pattern size determines the resistance through the surface-bulk interface, and the trench length determines the resistance through the trench. Thus the effects of the SB basically become smaller with increasing pattern size. As a result, no height change was observed inside a pattern which was 100 times larger than the circle in Fig. 1. Preliminary results for  $p$ -type samples were consistent with the SB model: larger height change for negative sample biases for this case, although it was not as clear as the  $n$ -type sample.

The tip-surface separation is determined as a function of the sample bias at a constant current, which means that the effective sample bias can be evaluated from the vertical tip position. For this purpose, bias dependences of the tip position ( $Z$ - $V$  curves) were measured for the surface both inside and outside the circle shown in Fig. 1. Figure 2(a) shows the  $Z$ - $V$  curves at a tunneling current of  $1.0$  nA. At positive sample bias, the tip approached the surface by approximately  $0.3$  nm outside the circle with a bias change from  $+2.0$  to  $+0.5$  V. On the other hand, the tip inside the circle was displaced by  $0.5$  nm, and the  $Z$ - $V$  curve became steeper. From these curves, the voltage drop can be derived by converting height change to voltage drop. An example for the case of a sample bias of  $1.5$  V is shown in Fig. 2(a).

The equivalent electric circuit for the circle is shown in the inset of Fig. 2(a), where  $R_{\text{tunnel}}$  is the tunneling resistance between the tip and the surface states and the thermionic current path of the SB is shown by a diode symbol. In the current-leakage model mentioned above, the voltage drop at a positive sample bias is given by the leakage resistance  $R_{\text{leak}}$  multiplied by the tunneling current. The bias dependence of the voltage drop [Fig. 2(b)] shows that the voltage drop is almost constant at  $0.47 \pm 0.02$  V, which corresponds to the reverse bias for the SB as shown in the schematic energy band diagrams in Fig. 2(b). For the case of this particular circle trench,  $R_{\text{leak}}$  is calculated as  $4.7 \times 10^8 \Omega$ , which is much smaller than that of the

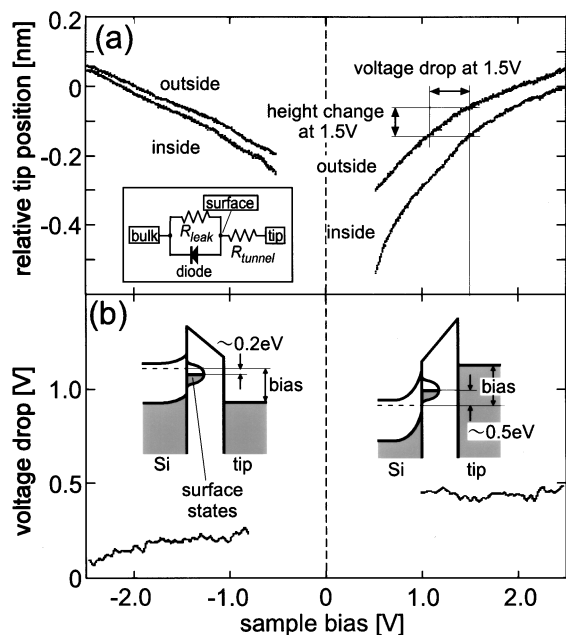


FIG. 2. (a) Z-V characteristics inside and outside the pattern at a constant current of 1.0 nA and (b) bias-voltage dependence of voltage drop of the inside region. The voltage drop is almost constant especially at positive bias. The equivalent circuit is shown in the inset of (a). Energy band diagrams are schematically shown in (b).

Schottky junction as a reversed bias of 0.5 V ( $10^{11} \Omega$ ) assuming a typical SB height of 0.55 eV. At a negative sample bias, the voltage drop again shows an almost constant value of approximately 0.2 V [Fig. 2(b)], although it slightly decreases with increasing sample bias. From this value, the total resistance between the surface inside the circle and the bulk is calculated to be approximately  $2 \times 10^8 \Omega$ . It is in good agreement with the combined resistance of  $R_{\text{leak}}$  and the SB resistance at a forward bias of 0.2 V ( $10^8$ - $\Omega$  range). These results show the validity of the current-leakage model for both the forward and reverse bias.

To investigate the leakage current paths when the SB is reverse biased, nested rectangular patterns of  $230 \text{ nm} \times 330 \text{ nm}$  and  $100 \text{ nm} \times 140 \text{ nm}$  were made. The voltage drop in the doubly surrounded region was approximately twice that in the singly surrounded region. This indicates that the current leak through the trench is dominating the  $R_{\text{leak}}$ .

The validity of the SB model can be reexamined here briefly based on the observed voltage drop, although the details will be discussed elsewhere [17]. The polarity dependence of the STM observation would be explained by the asymmetry in the electronic structures of the tip and the sample. However, the Z-V characteristics [Fig. 2(a)] already include the effects of the electronic structures, and nevertheless the voltage drop is almost constant except for the difference between negative and positive biases. Therefore, the asymmetry in the STM observation in Fig. 1 between occupied and unoccupied states should

be attributed to the asymmetry in the interface resistance between positive and negative sample biases. This is the major reason why we argue the SB model.

The insulating trench can be used to restrict the current leakage path. A tape structure, 18 nm in width and 390 nm in length, was fabricated by surrounding the surface with 20-nm-wide trenches. Figure 3(a) shows an STM image of the tape structure observed at a sample bias of  $-2.0 \text{ V}$ . Although the apparent height of the tape structure is 0.06 nm lower than the rest of the surface, it does not depend on the position. The result for a positive bias of 2.0 V is shown in Fig. 3(b). The apparent height of the surface becomes lower as the STM tip approaches the closed end of the structure, and the height change is saturated at approximately 0.2 nm. Using Z-V characteristics, the voltage drop along the tape structure is obtained as a function of lateral position [Fig. 3(c)]. To estimate the surface conductivity, we used a simple circuit model for the tape structure, consisting of a resistance  $R_S$  uniformly distributed in one dimension along the surface states, a leakage resistance  $R_L$  uniformly distributed between the surface states and the bulk, and a leakage resistance  $R_T$  between the closed end and the bulk. An equivalent circuit diagram is shown in the inset of Fig. 3(c), in which  $R_S$  and  $R_L$  are the total resistances. Since the current across the structure is negligible compared with the current along it, a one-dimensional model

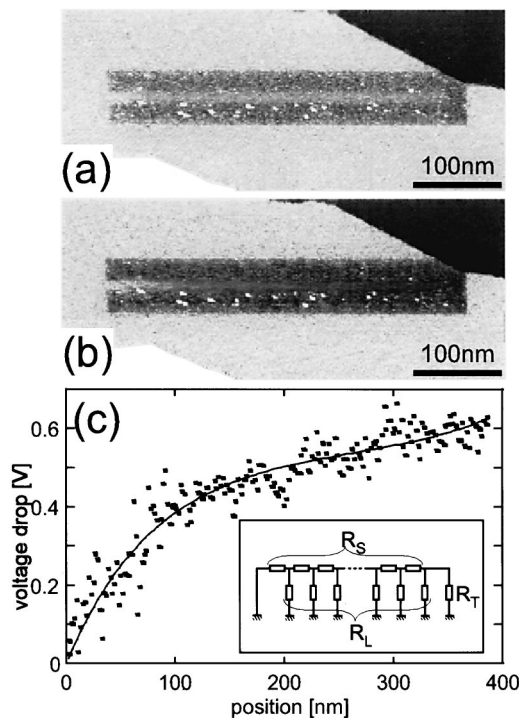


FIG. 3. Filled and empty STM images of tape structure observed at (a)  $-2.0 \text{ V}$  and (b)  $+2.0 \text{ V}$ . (c) Voltage drop along the tape structure for positive-bias observation derived from Z-V characteristics. The solid line is a calculated curve fitted to the experimental data using the electrical circuit model shown in the inset.

was adopted for this structure. The voltage drop can be calculated as a function of lateral position along the tape structure, at which the STM tip supplies a constant tunneling current. By adjusting these three parameters  $R_S$ ,  $R_L$ , and  $R_T$ , the function was fitted to the experiment, and the resulting curve is shown in Fig. 3(c). The obtained resistances are  $R_S = 2.5 \times 10^9 \Omega$ ,  $R_L = 4.6 \times 10^8 \Omega$ , and  $R_T = 1.5 \times 10^9 \Omega$ . The surface-state sheet conductivity estimated from  $R_S$  is  $8.7 \times 10^{-9} \Omega^{-1}\square$ .

A couple of works have been reported on conduction through surface states of Si(111)-(7 × 7). Using EELS data from Persson *et al.* [18] and Stroscio *et al.* [19] the surface-state conductivity was deduced to be in the  $10^{-5}\text{-}\Omega^{-1}\square$  range [3]. However, because the conductivity obtained by EELS is an ac conductivity, it may not be simply compared with our results. With point-contact measurement, Hasegawa *et al.* [7] reported a surface conductance in the  $10^{-6}\text{-}\Omega^{-1}$  range. Using the surface conductivity we obtained above and considering the current path through the surface-bulk interface, the point-contact conductance is estimated to be in the  $10^{-8}$  to  $10^{-7}\text{-}\Omega^{-7}$  range. Since they measured the conduction through the whole surface by pushing the tip into the surface, the measured value may include the conduction through the bulk, especially through the space-charge layer.

Hasegawa *et al.* [20] measured the surface conductivity of Si(111)-(7 × 7) by the four-probe method. During metal deposition, the conductivity increased by  $10^{-5}$  to  $10^{-4} \Omega^{-1}\square$ , which was attributed to the change of space-charge layer due to Fermi-level pinning. However, the conductivity of the clean surface was comparable to that of bulk, which indicates that the surface-state conductivity is negligibly small. Thus we can say that the surface-state conductivity should be much smaller than that through the space-charge layer. Photoemission spectra [21] and our tunneling spectra indicate that the surface-state bands originating from dangling bonds are quite narrow, suggesting the low conductivity due to the low mobility of the carriers in surface states.

There are two conceivable origins of the low mobility: the localization of carriers in the vicinity of the dangling bonds and the localization within the half unit cell of the (7 × 7) structure. In the DAS model [12], the half unit cell consists of nine dangling bonds of adatoms and rest atoms. First-principles calculation for a Si(111)-(7 × 7) surface showed a high density of electronic states only in the vicinity of dangling bonds near the Fermi energy [22], which suggests the possibility of charge localization around dangling bonds. Although the local density of states is relatively high within half unit cells, each half cell is separated by 0.66-nm-wide grooves including three dimers without dangling bonds. Therefore, electrons in dangling-bond states may be localized within the half cells. If we assume tunneling junctions for the current path between adjoining half cells and evaluate its value based on the first-principles calculation of the

correlation between the tunneling current and the tip-surface distance [23], the sheet conductivity is estimated to be in the  $10^{-8}\text{-}\Omega^{-1}\square$  range, which is comparable to our result. For a more precise estimation, however, theoretical calculations of the conductance within and between half cells are necessary. A detailed analysis will be published elsewhere [17].

In conclusion, the effects of the natural SB between the surface states and the bulk states of the Si(111)-(7 × 7) surface were directly observed using an STM surface modification technique. When a surface was surrounded by insulating trenches, effective sample bias was reduced inside the pattern due to a high resistance of the reverse-biased SB. Results of tunneling spectroscopy indicated rectifying characteristics inside the pattern. By measuring the voltage drop along a fabricated tape structure, the surface-state conductivity was evaluated to be  $8.7 \times 10^{-9} \Omega^{-1}\square$ , which is orders of magnitude lower than those reported previously.

- 
- [1] M. Henzler, *Surface Physics of Materials* (Academic Press, New York, 1975).
  - [2] D. E. Aspnes and P. Handler, *Surf. Sci.* **4**, 353 (1966).
  - [3] B. N. J. Persson, *Phys. Rev. B* **34**, 5916 (1986).
  - [4] G. Binnig, H. Rohrer, Ch. Gerber, and E. Weibel, *Phys. Rev. Lett.* **49**, 57 (1982).
  - [5] Y. Hasegawa and Ph. Avouris, *Phys. Rev. Lett.* **71**, 1071 (1993).
  - [6] D. M. Eigler and E. K. Schweizer, *Nature (London)* **344**, 524 (1990).
  - [7] Y. Hasegawa, I. W. Lyo, and Ph. Avouris, *Appl. Surf. Sci.* **76/77**, 347 (1994).
  - [8] S. Heike *et al.*, *Jpn. J. Appl. Phys.* **35**, L1367 (1996).
  - [9] R. Guckenberger *et al.*, *Science* **266**, 1538 (1994).
  - [10] J. Bardeen, *Phys. Rev.* **71**, 717 (1947).
  - [11] T. Komeda, R. Hasunuma, H. Mukaida, and H. Tokumoto, *Appl. Phys. Lett.* **68**, 3482 (1996).
  - [12] K. Takayanagi *et al.*, *J. Vac. Sci. Technol. A* **3**, 1502 (1985).
  - [13] R. Wolkow and Ph. Avouris, *Phys. Rev. Lett.* **60**, 1049 (1988).
  - [14] H. A. Bethe, MIT Radiation Laboratory Report No. 43-12, 1942.
  - [15] W. J. Kaiser and L. D. Bell, *Phys. Rev. Lett.* **60**, 1406 (1988).
  - [16] K. Kobayashi, *Phys. Rev. B* **57**, 12456 (1998).
  - [17] S. Heike *et al.* (unpublished).
  - [18] B. N. J. Persson and J. E. Demuth, *Phys. Rev. B* **30**, 5968 (1984).
  - [19] J. A. Stroscio and W. Ho, *Phys. Rev. Lett.* **54**, 1573 (1985).
  - [20] S. Hasegawa and S. Ino, *Phys. Rev. Lett.* **68**, 1192 (1992).
  - [21] J. E. Demuth, B. N. J. Persson, and A. J. Schell-Sorokin, *Phys. Rev. Lett.* **51**, 2214 (1983).
  - [22] H. Lim *et al.*, *Phys. Rev. B* **52**, 17231 (1995).
  - [23] N. Kobayashi, K. Hirose, and M. Tsukada, *Jpn. J. Appl. Phys.* **35**, 3710 (1996).